Wind Turbine Model and Observer in Takagi-Sugeno Model Structure

Sören Georg[1], Matthias Müller[1,2] and Horst Schulte[1]

[1] HTW Berlin, Department of Engineering I, Control Engineering, Berlin, Germany
[2] Key Wind Energy GmbH, Berlin, Germany

E-mail: soeren.georg@htw-berlin.de, horst.schulte@htw-berlin.de

Abstract. Based on a reduced-order, dynamic nonlinear wind turbine model in Takagi-Sugeno (TS) model structure, a TS state observer is designed as a disturbance observer to estimate the unknown effective wind speed. The TS observer model is an exact representation of the underlying nonlinear model, obtained by means of the sector-nonlinearity approach. The observer gain matrices are obtained by means of a linear matrix inequality (LMI) design approach for optimal fuzzy control, where weighting matrices for the individual system states and outputs are included. The observer is tested in simulations with the aero-elastic code FAST for the NREL 5 MW reference turbine, where it shows a stable behaviour in turbulent wind simulations.

1. Introduction

Takagi-Sugeno (TS) models provide a useful and uniform framework for nonlinear controller and observer design for dynamic systems. Originally introduced in the context of fuzzy systems [1], TS models are weighted combinations of linear submodels and can either be derived from input-output data via system identification [1, 2] or from mathematical models of nonlinear systems. Methods based on solving linear matrix inequalities (LMIs) allow for implicit stable controller and observer design for TS models [3, 4, 5].

In this paper, a TS observer is designed as a disturbance observer to estimate the unknown effective wind speed from the available measurable system outputs. This observer has been used along with a fault reconstruction and fault-tolerant control module, where the wind speed is needed as an input signal [6, 7].

Other methods have been applied to wind speed estimation in the literature. See for example [8], where Kalman filtering, extended Kalman filtering and the Newton-Raphson method are used and compared. Other dedicated algorithms have been applied, too. In [9], a state-observer for the rotor speed is combined with a PI controller to estimate the aerodynamic rotor torque. The effective wind speed is then reconstructed from the estimated torque signal via inversion of the aerodynamic model. While being able to yield good wind speed estimates, these methods also have certain detriments. The Kalman Filter is only applicable to linear state-space models. Thus, estimating the wind speed for a wind turbine using a Kalman Filter only yields good results in the region of one operating point of a linearised wind turbine model. A possible remedy is provided by the extended Kalman filter, however, it is not possible to verify formal stability for the error dynamics, since the extended Kalman filter is an adaptive method.

By contrast, for observers in TS structure, the formal stability of the error dynamics can, at least in principle, be shown using linear matrix inequalities (LMI). The TS observer structure can also be extended to a TS sliding mode observer used for fault reconstruction [10, 6, 7]. For these reasons, and to achieve a certain level of uniformity within the design methods for different modules of a fault-tolerant control scheme, an observer in TS structure is used here for the estimation of the effective wind speed.

This paper is organised as follows. In section 2, the reduced-order wind turbine model is introduced. In section 3, the TS model structure is introduced along with an illustrating example. The observer is derived in TS structure and the method to obtain the observer gain matrices is discussed. Simulation results are presented in section 4.

2. Wind Turbine Model

For the purpose of model-based control design, reduced-order models like those in [11, 12] are appropriate, since they capture only the dominant system dynamics that are directly influenced by the control action [12]. A reduced-order model inspired from [12], which was derived in TS structure in [13], is briefly introduced in this section and serves as a basis for the observer design in section 3. Furthermore, the model is used as a simulation environment. Additionally, the aero-elastic code FAST by NREL [14] is used for the simulation studies, in order to test the observer with a more realistic wind turbine model (see section 4).

Four degrees of freedom are considered for the reduced-order model: rotor and generator rotation angles (θ_r, θ_g), fore-aft tower top deflection y_T and flapwise blade tip deflection y_B. The equations of motion, which describe the dynamics of the mechanical model, are obtained as

$$\begin{aligned}
(m_T + N m_B)\,\ddot{y}_T + N m_B\,\ddot{y}_B + d_T\,\dot{y}_T + k_T\,y_T &= F_T && (1)\\
N m_B\,\ddot{y}_T + N m_B\,\ddot{y}_B + N d_B\,\dot{y}_B + N k_B\,y_B &= F_T && (2)\\
J_r\,\dot{\omega}_r + d_S\,(\omega_r - \omega_g) + k_S\,\theta_s &= T_a && (3)\\
J_g\,\dot{\omega}_g - d_S\,(\omega_r - \omega_g) - k_S\,\theta_s &= -T_g\,, && (4)
\end{aligned}$$

where N denotes the number of rotor blades, R the rotor radius, m_T and m_B the effective tower and blade masses, k_T and k_B the effective stiffness coefficients for the tower top and blade tip deflection, d_T and d_B the damping coefficients for the respective tower and blade dynamics. $\theta_s = \theta_r - \theta_g$ denotes the shaft torsion angle, ω_r and ω_g the rotor and generator speed respectively. F_T and T_a denote the aerodynamic rotor thrust and torque respectively and T_g the applied generator torque. An ideal gearbox is assumed, where the gearbox ratio is set to 1 for reasons of simplicity.

A lateral tower bending is not considered here. Furthermore, the effect of gravity on the blade bending is neglected. These assumptions are common when using reduced-order models for controller or observer design [12].

In Equation 2, the dynamics of all N blades is treated equally, i.e., a uniform blade dynamics, reflected in only one deflection degree of freedom y_B is considered. As a consequence, collective pitch is considered. The (collective) pitch dynamics can be incorporated into the wind turbine model as a first-order delay model, $\tau_\beta\,\dot{\beta} + \beta = \beta_d$, where β_d denotes the demanded pitch angle and τ_β the delay time constant.

Introducing the state vector $\mathbf{x} = (y_T \quad y_B \quad \theta_s \quad \dot{y}_T \quad \dot{y}_B \quad \omega_r \quad \omega_g \quad \beta)^T$ and the input vector $\mathbf{u} = (\beta_d \quad T_g)^T$ of the two actuator signals, the system of dynamic equations (1) to (4) including the pitch dynamics can be transformed into a state-space form:

$$\dot{x}_1 = x_4 \tag{5}$$
$$\dot{x}_2 = x_5 \tag{6}$$
$$\dot{x}_3 = x_6 - x_7 \tag{7}$$
$$\dot{x}_4 = \tfrac{1}{m_T}\left(-k_T\,x_1 + N\,k_B\,x_2 - d_T\,x_4 + N\,d_B\,x_5\right) \tag{8}$$
$$\dot{x}_5 = \tfrac{k_T}{m_T}\,x_1 - \tfrac{m_T+Nm_B}{m_B\,m_T}\,k_B\,x_2 + \tfrac{d_T}{m_T}\,x_4 - \left(\tfrac{1}{m_B}+\tfrac{N}{m_T}\right)d_B\,x_5 + \tfrac{1}{Nm_B}\,F_T \tag{9}$$
$$\dot{x}_6 = -\tfrac{1}{J_r}\left(d_S\,(x_6 - x_7) + k_S\,x_3\right) + \tfrac{1}{J_r}\,T_a \tag{10}$$
$$\dot{x}_7 = \tfrac{1}{J_g}\left(d_S\,(x_6 - x_7) + k_S\,x_3\right) - \tfrac{1}{J_g}\,u_2 \tag{11}$$
$$\dot{x}_8 = -\tfrac{1}{\tau}\,x_8 + \tfrac{1}{\tau}\,u_1\,, \tag{12}$$

which can also be written in matrix form as

$$\dot{\mathbf{x}} = \mathbf{A}\,\mathbf{x} + \mathbf{B}\,\mathbf{u} + \mathbf{g}(\mathbf{x}, v)\,, \tag{13}$$

with system matrix $\mathbf{A}$, input matrix $\mathbf{B}$ and a nonlinear state vector $\mathbf{g}(\mathbf{x}, v)$ [13].
The aerodynamic rotor thrust and torque are given by $F_T = \frac{\rho\pi R^2}{2}\,C_T\,(\lambda,\beta)\;v^2$ and $T_a = \frac{\rho\pi R^3}{2}\,C_Q\,(\lambda,\beta)\;v^2$, where R denotes the rotor radius, ρ the air density, v the wind speed and $\lambda = R\,\frac{\omega_r}{v}$ the tip speed ratio. C_Q and C_T are the aero maps for the rotor thrust and torque coefficients. Due to the expressions for F_T and T_a, the state-space model (13) is nonlinear.

2.1. Model Parameters

The model parameters for the turbine model (13) are based on the NREL 5 MW reference turbine [15]. The parameters are listed in Appendix B, some of which can be directly taken from [15] or example input and log files of FAST simulation runs of the 5 MW reference turbine.

2.1.1. Structural Parameters The dynamics of fore-aft tower bending and flap-wise rotor blade bending are reduced to simple spring-mass-damper systems for the tower top and blade tip deflections. The respective tower stiffness coefficient k_T is derived by means of a direct stiffness method common in structural mechanics calculations. The tower consisting of several segments is first transformed into an equivalent bending beam model. Afterwards, the bending stiffness of the effective beam model is transformed to an equivalent translational stiffness of the tower-nacelle dynamics (see Appendix A).
While the tower stiffness parameter could be obtained and validated against the FAST simulation of the 5 MW reference turbine, there are still uncertainties about the determination of the blade parameter k_B, which is therefore adjusted according to FAST simulation results [13].

The effective mass m_T for the tower-nacelle motion in equations (8), (9)) is estimated as $m_T = m_{\text{Rotor}} + m_{\text{Nacelle}} + 0.25\,m_{\text{Tower}}$, which has proven a reasonable assumption [16]. Similarly, the effective blade mass for the blade tip motion is estimated as $m_B = 0.25\,m_{\text{Blade}}$.

2.1.2. Aerodynamic Damping The aerodynamic rotor damping in fore-aft direction, which can be approximated as $d_{11}\,(\lambda,\beta) = 0.5\,\rho\,\pi\,R^2\,v\,d^*_{11}\,(\lambda)$ [17], is taken as an estimate for the damping parameter d_T of the tower-top motion in equations (8), (9). The dimensionless parameter $d^*_{11}\,(\lambda,\beta)$ depends on the tip speed ratio and on the pitch angle and shows a similar behaviour for different turbine sizes [17]. Estimating $d_{11}\,(\lambda,\beta)$ accordingly for different stationary points of the 5 MW reference turbine for the whole operating range of the turbine yields values between

$3 \cdot 10^4 \frac{\text{Ns}}{\text{m}}$ and $10 \cdot 10^4 \frac{\text{Ns}}{\text{m}}$. Here, the tower damping parameter is set to a constant value of $d_T = 7 \cdot 10^4 \frac{\text{Ns}}{\text{m}}$. The blade damping parameter is set to $d_B = 2 \cdot 10^4 \frac{\text{Ns}}{\text{m}}$.

2.1.3. Aero Maps The aero maps for the rotor thrust (C_T) and torque coefficients (C_Q) were extracted from FAST simulation runs of the 5 MW reference turbine [13]. Alternatively, they can be approximated using nonlinear functions [13].

3. Observer in Takagi-Sugeno Model Structure

In this section, a state-observer based on the nonlinear model (13) is designed to reconstruct the unknown wind speed from the measurable system states. The standard Luenberger observer for linear systems is a state-space model including a feedback of the output error $\mathbf{e_y} = \mathbf{y} - \widehat{\mathbf{y}}$, where $\widehat{\mathbf{y}}$ is the reconstructed output signal:

$$\dot{\widehat{\mathbf{x}}} = \mathbf{A}\,\mathbf{x} + \mathbf{B}\,\mathbf{u} + \mathbf{L}\,(\mathbf{y} - \widehat{\mathbf{y}})\,, \qquad \widehat{\mathbf{y}} = \mathbf{C}\,\widehat{\mathbf{x}}\,. \tag{14}$$

As the wind turbine model is nonlinear, a linear observer like (14) cannot be used in the whole operating range. Therefore, an observer in Takagi-Sugeno model structure is used.
A state-space model in TS structure is of the form

$$\dot{\mathbf{x}} = \sum_{i=1}^{N_r} h_i(\mathbf{z})\ (\mathbf{A}_i\,\mathbf{x} + \mathbf{B}_i\,\mathbf{u})\,, \qquad \mathbf{y} = \sum_{i=1}^{N_r} h_i(\mathbf{z})\,\mathbf{C}_i\,\mathbf{x}\,, \tag{15}$$

where $\mathbf{A}_i$, $\mathbf{B}_i$ and $\mathbf{C}_i$ are constant matrices and h_i are nonlinear functions of the premise variables $\mathbf{z}$, which can depend on the system states and inputs and on external variables. N_r denotes the number of linear submodels. The membership functions h_i fulfill the relation $\sum_{i=1}^{N_r} h_i = 1$. The linear submodels can be derived from the original nonlinear model using local Taylor linearisation or by applying the sector nonlinearity approach [18, 4], whereby an exact representation of the nonlinear model is obtained. This approach is used in this paper for the derivation of the TS observer model.

3.1. Illustrating Example for a TS-Model
A simple example shall be considered in order to illustrate the derivation of a TS model using sector nonlinearities.
Consider the dynamic equation of a pendulum of length l with a point mass m driven by an external torque signal M:

$$\ddot{\varphi} = -\frac{g}{l}\,\sin\,\varphi + \frac{1}{m\,l^2}\,M\,, \tag{16}$$

where φ denotes the angular displacement of the pendulum and g the gravitational constant.

Introducing the state vector $\mathbf{x} = (\varphi \quad \dot{\varphi})^T$ and the input signal $u = M$, equation (16) can be written in state-space form as

$$\dot{\mathbf{x}} = \begin{pmatrix} 0 & 1 \\ -\frac{g}{l}\,\frac{\sin\,x_1}{x_1} & 0 \end{pmatrix} \mathbf{x} + \begin{pmatrix} 0 \\ \frac{1}{m\,l^2} \end{pmatrix} u = \mathbf{A}\,(\mathbf{x})\,\mathbf{x} + \mathbf{B}\,u\,. \tag{17}$$

Obviously, this is a nonlinear model due to the function $f\,(x_1) = -\frac{g}{l}\,\frac{\sin\,x_1}{x_1}$. This function can be written as

$$f\,(x_1) = w_1\,(x_1)\,\overline{f} + w_2\,(x_1)\,\underline{f}\,, \text{ where } w_1\,(x_1) := \frac{f\,(x_1) - \underline{f}}{\overline{f} - \underline{f}}\,,\ w_2\,(x_1) := \frac{\overline{f} - f\,(x_1)}{\overline{f} - \underline{f}}\,.$$

$\overline{f}$ and $\underline{f}$ denote the maximum and minimum values of the function f, i.e. the sector boundaries. However, any real constants c_1, c_2 could be used instead, as long as $c_1 \neq c_2$. Using the sector boundaries is advantageous, since the matrices of the linear submodels, which are used for TS controller and observer design, thereby contain the domain of the nonlinear system.

From the definition of w_1 and w_2 it is obvious that $w_1 + w_2 = 1$. Thus, the nonlinear matrix $\mathbf{A}$ in (17) can be written as

$$\mathbf{A}\,(\mathbf{x}) \;=\; \begin{pmatrix} 0 & w_1 + w_2 \\ w_1\,\overline{f} + w_2\,\underline{f} & 0 \end{pmatrix} \;=\; w_1 \begin{pmatrix} 0 & 1 \\ \overline{f} & 0 \end{pmatrix} \;+\; w_2 \begin{pmatrix} 0 & 1 \\ \underline{f} & 0 \end{pmatrix} \;=\; w_1\,\mathbf{A}_1 \;+\; w_2\,\mathbf{A}_2\,, \qquad (18)$$

and the whole model in (17) as $\dot{\mathbf{x}} = \sum_{i=1}^{2} w_i(x_1)\;(\mathbf{A}_i\,\mathbf{x} + \mathbf{B}\,u)$.
The nonlinearity has thus been shifted from the system matrix into the membership functions, which in this case are equivalent to the weighting functions w_i. In the same manner, systems with more than one nonlinearity can be transformed into a TS model structure by including all possible permutations of the w_i-functions into the membership functions h_i. The number N_r of linear submodels generally is $N_r = 2^{N_l}$, where N_l is the number of distinct nonlinear functions. However, if there occur several linear combinations of the same nonlinear function, N_l is not increased.

3.2. TS Observer

The state-space model (13) is used as a basis for the observer, where either the full model (13) or submodels of (13) can be used depending on the desired observer model order.

In this paper, only the rotational degree of freedom is incorporated into the observer model but no torsional, tower and blade dynamics. This model configuration for the observer yields reasonable results while requiring only the rotor speed as a measurement signal. An extension of the observer model to include the torsional degree of freedom yields only minor differences in the simulation results and requires a measurement of the torsion angle, which may be difficult to achieve for a turbine with gearbox.
In order to estimate the wind speed v with a state observer, v is included into the system state vector $\mathbf{x}$ and a dynamic wind model is added to the system equations. The first-order delay model from [19] is used, modified by the mean value $\bar{v}$ of the wind speed, but without a white noise term:

$$\dot{v} \;=\; -\frac{1}{\tau_v}\;(v - \bar{v})\;, \qquad (19)$$

where the time constant is estimated as $\tau_v = 4\,\mathrm{s}$. The mean wind speed $\bar{v}$ can be calculated over an appropriate time period (e.g. 10 min) from the anemometer wind measurement, which is sufficient for this purpose.

Since only the rotational degree of freedom plus the estimated wind speed are considered for the observer model, the corresponding estimated state vector is $\widehat{\mathbf{x}} = (\hat{\omega}_r \quad \hat{v})^T$. Since the first order pitch dynamics adds no information as to the reconstruction of the unknown states, it is not considered in the observer model. This implies that the demanded pitch angle β_d is not included in the input vector, because there is no linear dependence on β_d but only a nonlinear dependence in $C_Q\left(\hat{\lambda}, \beta_d\right)$. The mean wind speed $\bar{v}$ can be included in the input vector: $\mathbf{u} = (T_g \quad \bar{v})^T$. The output vector contains only the rotor speed: $\mathbf{y} = y = \omega_r$ and the output matrix is given by $\mathbf{C} = (1 \quad 0)$. For a real application of the observer, the rotor speed signal would either have to be measured with high resolution, for example by means of optical

scanning of nearly continuous barcodes on the main shaft. Alternatively, in a wind turbine with gearbox, the generator speed signal (corrected by the gearbox ratio) could be used instead.

From the system of nonlinear state-space equations for the wind turbine model (13), it is straightforward to obtain the nonlinear system matrix and the input matrix for the observer model including only the rotational degree of freedom and the wind speed:

$$\mathbf{A}\left(\mathbf{x}\right) = \begin{pmatrix} 0 & f\left(\widehat{\mathbf{x}},\, \beta_d\right) \\ 0 & -\frac{1}{\tau_v} \end{pmatrix}, \quad \mathbf{B} = \begin{pmatrix} -\frac{1}{J_r+J_g} & 0 \\ 0 & \frac{1}{\tau_v} \end{pmatrix}, \tag{20}$$

where the nonlinear function f and its minimum and maximum values are given by
$f\left(\widehat{\mathbf{x}},\, \beta_d\right) = \frac{1}{2\,J_r}\,\rho\,\pi\,R^3\,\hat{v}\,C_Q\left(\hat{\lambda}, \beta_d\right)$, $\quad \underline{f} = 1.1 \cdot 10^{-5}\,\frac{1}{\mathrm{m\,s}}$, $\quad \overline{f} = 0.0495\,\frac{1}{\mathrm{m\,s}}$.
The values for $\underline{f}$ and $\overline{f}$ were obtained by estimating the minimum and maximum values of the wind speed v and the torque coefficient C_Q: $C_{Q,\max} = 0.0751$, $C_{Q,\min} = 0.001$, $v_{\max} = 60\,\frac{\mathrm{m}}{\mathrm{s}}$, $v_{\min} = 1\,\frac{\mathrm{m}}{\mathrm{s}}$. Though $v_{\min}$ and $C_{Q,\min}$ are zero in theory, they are set to small positive values to avoid generating zero entries in one of the TS submatrices.

Employing the same procedure as in section 3.1, the observer model can be obtained in TS structure:

$$\dot{\widehat{\mathbf{x}}} = \sum_{i=1}^{N_r=2} h_i(\widehat{\mathbf{z}})\,\left(\mathbf{A}_i\,\widehat{\mathbf{x}} + \mathbf{B}\,\mathbf{u} + \mathbf{L}_i\left(\mathbf{y} - \widehat{\mathbf{y}}\right)\right), \qquad \widehat{\mathbf{y}} = \mathbf{C}\,\widehat{\mathbf{x}}, \tag{21}$$

where the premise variable $\widehat{\mathbf{z}}$ now depends on the reconstructed states: $\widehat{\mathbf{z}} = \left(\hat{\omega}_r\ \hat{v}\ \beta_d\right)^T$.

3.3. Observer Gains and Stability

A common means to derive gain matrices for observers in TS structure is by applying the direct method of Lyapunov in form of linear matrix inequalities (LMI) [5].

In general, the global asymptotic stability of a nonlinear system $\dot{\mathbf{x}} = \mathbf{f}\left(\mathbf{x}\right)$ is guaranteed if there exists a Lyapunov function $V\left(\mathbf{x}\right)$ satisfying the conditions $V\left(\mathbf{x}\right) > 0$ and $\dot{V}\left(\mathbf{x}\right) < 0$ for all trajectories. In particular, the system is stable if it is quadratically stable, i.e., if a quadratic Lyapunov function $V = \mathbf{x}^T\mathbf{P}\mathbf{x}$, with a symmetric, positive definite matrix $\mathbf{P}$, exists.
In that case, for a TS system without an external input ($\dot{\mathbf{x}} = \sum_{i=1}^{N_r} h_i\left(\mathbf{z}\right)\,\mathbf{A}_i$), the condition $\dot{V}\left(\mathbf{x}\right) < 0$ is equivalent to $\dot{V} = \dot{\mathbf{x}}^T\,\mathbf{P}\,\mathbf{x} + \mathbf{x}^T\,\mathbf{P}\,\dot{\mathbf{x}} = \mathbf{x}^T\,\left(\sum_{i=1}^{N_r} h_i\left(\mathbf{z}\right)\,\left(\mathbf{A}_i^T\,\mathbf{P} + \mathbf{P}\,\mathbf{A}_i\right)\right)\,\mathbf{x} < 0$. Since this condition must hold for all $\mathbf{x}$, the TS system without input is stable if there exists a common symmetric, positive definite matrix $\mathbf{P}$, such that

$$\mathbf{A}_i^T\,\mathbf{P} + \mathbf{P}\,\mathbf{A}_i < 0 \qquad \left(i \in \{1, \ldots, N_r\}\right). \quad [20,\ 3] \tag{22}$$

For the TS observer (21), where the membership functions depend on unmeasurable states ($h_i = h_i\left(\widehat{\mathbf{z}}\right)$), a modified form of the stability condition (22) with an additional LMI can be used to guarantee the stability of the error dynamics of the observer system [21]:

$$\mathbf{P}\,\left(\mathbf{A}_i - \mathbf{L}_i\mathbf{C}\right) + \left(\mathbf{A}_i - \mathbf{L}_i\mathbf{C}\right)^T\,\mathbf{P} \leq -\mathbf{Q}, \qquad \begin{pmatrix} \mathbf{Q} & -\mu^2 I & \mathbf{P} \\ & \mathbf{P} & \mathbf{I} \end{pmatrix} > 0, \tag{23}$$

where $\mathbf{Q}$ is a symmetric, positive definite matrix and $\mu > 0$ is a known constant satisfying $\Delta\left(\mathbf{z}, \widehat{\mathbf{z}}\right) \leq \mu\|\mathbf{e}\|$, with $\mathbf{e} = \|\mathbf{x} - \widehat{\mathbf{x}}\|$ and $\Delta\left(\mathbf{z}, \widehat{\mathbf{z}}\right) = \left\|\sum_{i=1}^{N_r}\left(h_i(\mathbf{z}) - h_i(\widehat{\mathbf{z}})\right)\left(\mathbf{A}_i\mathbf{x} + \mathbf{B}\mathbf{u}\right)\right\|$. The first inequality of (23) is not an LMI but can be recast in LMI form by introducing $\mathbf{N}_i := \mathbf{P}\mathbf{L}_i$ [4]. As condition (23) concerns quadratic stability, it is only a sufficient stability condition, i.e.,

if it is not fulfilled, no formal statement can be made about the stability or instability of the considered system [5].

Optimal LMI Observer Design Condition (23) was first used to calculate the observer gains. However, this observer hardly had any modifying effect on the wind speed compared to the mere wind model (19). A possible remedy is to modify the gain matrices with a weighting matrix, such that the gains influencing the wind speed $\hat{v}$ are increased. A more systematic way is to make use of optimal fuzzy control concepts, where weighting matrices for the system states/outputs and inputs and a quadratic cost function can be included in the LMIs [22].
For the observer design in this paper, theorem 5 from [22], which is applicable for controller design, was modified to be used for the dual TS-systems $\left(\mathbf{A}_i^T, \mathbf{C}^T\right)$. The observer gain matrices $\mathbf{L}_i$ are then obtained from the resulting gain matrices $\mathbf{K}_i$ as $\mathbf{L}_i = \mathbf{K}_i^T$. The obtained gain matrices are given in Appendix C.

The formal stability of the error dynamics could not be verified with condition (23), which is a conservative condition due to the assumption of un unstructured uncertainty [5]. However, the observer shows a stable behaviour in the FAST simulation, even for large initial observer errors (see section 4, Figure 2).

4. Simulation Results

The observer was tested in turbulent wind simulations with both the nominal model (13) and FAST. To control the rotor speed, a state-space controller in TS structure, based on Taylor-linearised models was used [7]. To examine the observer in different regions, simulations were conducted with mean wind speeds of 8, 18, and 24 m/s. In Figure 1, results are shown for a mean wind speed of 18 m/s. One can see that in both simulation models, an almost perfect reconstruction is achieved for the rotor speed. For the wind speed, a pretty good reconstruction is achieved in the nominal model simulation (see Figure 1a), where only very fast changes and peaks are not reflected in the reconstructed wind speed. When looking at the wind speed reconstruction in the FAST simulation (Figure 1c), the reconstruction quality is seemingly inferior. However, when interpreting Figure 1c, it is important to remember that the observer estimates the rotor effective wind speed, i.e. a virtual single point wind speed that causes the same variations in wind torque as the corresponding 3D turbulent wind field [23]. Although the calculations in FAST are based on the 3D wind field, the wind speed output from FAST (blue curve in Figure 1c) shows the nominal downwind component of the hub-height wind speed, so the two wind speed curves in Figure 1c are not directly comparable. The direct comparison of Figures 1a and 1c shows that the influence of the 3D wind field in the FAST simulation leads to an averaging effect compared to the nominal model simulation, where a uniform (hub-height) wind speed acts on the rotor.

The results in Figure 1 were obtained using the same initial rotor speed values for the simulation model and the observer. To further test the observer stability, a simulation was conducted with larger initial observer errors (see Figure 2). As can bee seen, apart from a larger initial transient peak in the reconstructed wind speed, a stable observer behaviour is still obtained.

Two further simulations were conducted with mean wind speeds of 24 m/s (Figure 3) and 8 m/s (Figure 4). In both cases, the same pattern can be observed that the difference between the reconstructed wind speed and the hub-height reference wind speed is much larger in FAST simulations than in the nominal model simulations, which is due to the averaging effect of the 3D wind field in FAST.

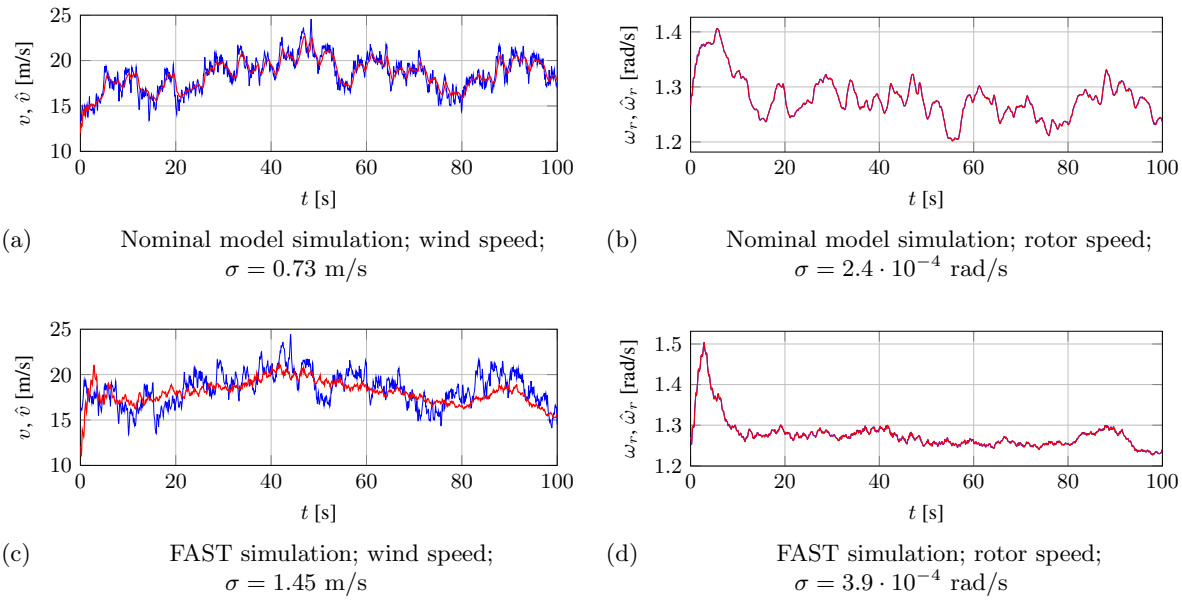

(a) Nominal model simulation; wind speed; $\sigma = 0.73$ m/s

(b) Nominal model simulation; rotor speed; $\sigma = 2.4 \cdot 10^{-4}$ rad/s

(c) FAST simulation; wind speed; $\sigma = 1.45$ m/s

(d) FAST simulation; rotor speed; $\sigma = 3.9 \cdot 10^{-4}$ rad/s

Figure 1. Turbulent wind simulations (mean wind speed: 18 m/s, turbulence intensity: 15 % (NTM), Kaimal model). Blue: states from simulation; red: estimated states; initial values: $\omega_{r,0} = \hat{\omega}_{r,0} = 1.267\,\text{rad/s}$, $\hat{v}_0 = 12\,\text{m/s}$. σ denotes the standard deviation between the simulation states and the estimated values.

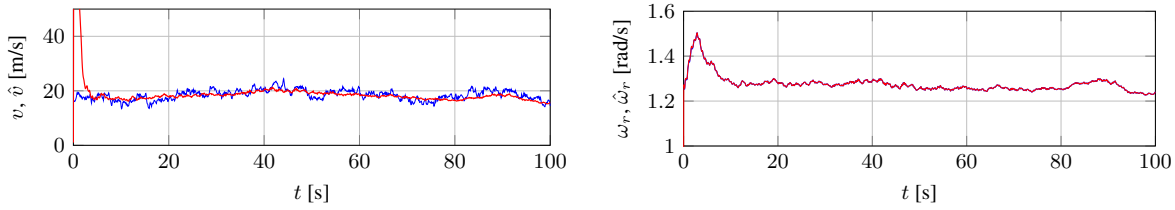

(a) Wind speed; $\sigma = 6.5$ m/s

(b) Rotor speed; $\sigma = 0.014$ rad/s

Figure 2. FAST simulation with turbulent wind (mean wind speed: 18 m/s, turbulence intensity: 15 % (NTM), Kaimal model). Blue: states from simulation; red: estimated states; initial values: $\omega_{r,0} = 1.267\,\text{rad/s}$, $\hat{\omega}_{r,0} = 0\,\text{rad/s}$, $\hat{v}_0 = 1\,\text{m/s}$. The initial peak in the reconstructed wind speed is not fully shown here, in order to keep the differences between v and $\hat{v}$ visible in the rest of the time-series.

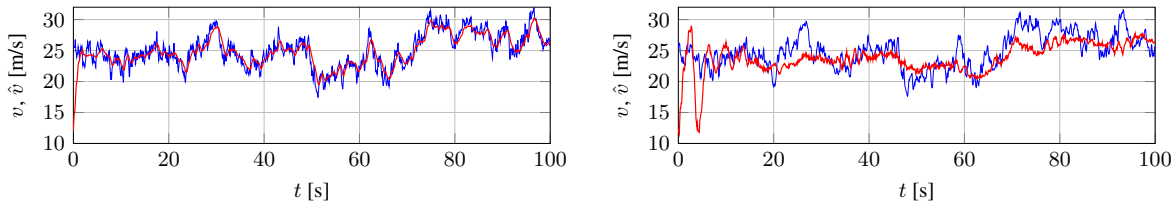

(a) Nominal model simulation; $\sigma = 1.3$ m/s

(b) FAST simulation; $\sigma = 2.5$ m/s

Figure 3. Turbulent wind simulations (mean wind speed: 24 m/s, turbulence intensity: 14 % (NTM), Kaimal model). Blue: wind speed from simulation; red: estimated wind speed; initial values: $\omega_{r,0} = \hat{\omega}_{r,0} = 1.267\,\text{rad/s}$, $\hat{v}_0 = 12\,\text{m/s}$.

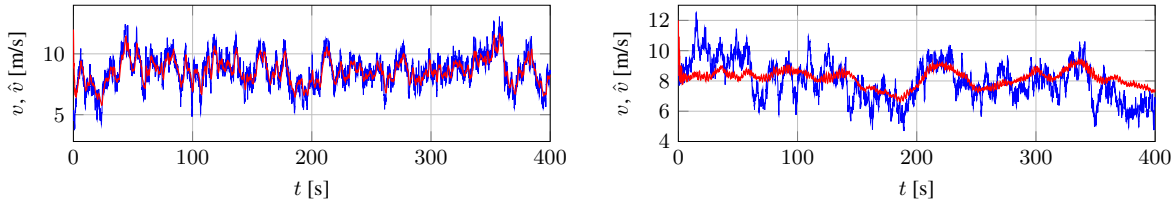

(a) Nominal model simulation; $\sigma = 0.8$ m/s (b) FAST simulation; $\sigma = 1.3$ m/s

Figure 4. Turbulent wind simulations (mean wind speed: 8 m/s, turbulence intensity: 20 % (NTM), Kaimal model). Blue: wind speed from simulation; red: estimated wind speed; initial values: $\omega_{r,0} = \hat{\omega}_{r,0} = 1.267\,\mathrm{rad/s}$, $\hat{v}_0 = 12\,\mathrm{m/s}$.

5. Conclusion

In this paper, a nonlinear observer in Takagi-Sugeno structure was designed to estimate the effective wind speed from the measurable states of a dynamic wind turbine model. Although formal stability of the observer in terms of LMI conditions could not be obtained, the observer shows a stable behaviour when used with the aero-elastic simulation code FAST. The observer yields reasonable wind speed reconstruction results in the complete operating region of a wind turbine, although the reconstruction quality slightly decreases for lower wind speeds.

Acknowledgments

This work was conducted within a research project funded by the German Federal Ministry of Education and Research under grant no. 17N1411.

Appendix A. Derivation of Effective Tower Stiffness

The direct stiffness method allows to calculate eigenfrequencies and eigenmodes of structures consisting of several segments of defined length, mass and bending stiffness. For each segment, the characteristic forces and displacements can be calculated from the previous segment by means of a transfer matrix depending on the frequency of the structure [24]. Applying the total transfer matrix as the product of the individual transfer matrices, as well as the boundary conditions for the rigid and the free ends of the beam, yields a homogeneous system of equations for the displacements at the top of the total structure, which is fulfilled for the eigenfrequencies of the structure. In order to calculate the respective equivalent bending stiffness, it is sufficient to find the first eigenfrequency ω_1. For the tower, it was calculated as $\omega_1 \approx 2.14\,\frac{\mathrm{rad}}{\mathrm{s}}$ and has been validated with the NREL-Software BModes [25] ($\omega_{1,\mathrm{BModes}} \approx 2.08\,\frac{\mathrm{rad}}{\mathrm{s}}$). The connection to the equivalent bending stiffness B_{total} is

$$\omega_1 = \kappa_1^2 \sqrt{\frac{B_{total}}{\mu_{total}}} \quad \Rightarrow \quad B_{total} = \frac{\omega_1^2\,\mu_{total}}{\kappa_1^4} \approx 4.44 \cdot 10^{11}\,\mathrm{Nm}^2\,, \tag{A.1}$$

where $\kappa_1 = 1.423 \cdot 10^{-2}$ is a factor that can be found in standard mechanics textbooks and μ_{total} is the total mass per length. Finally, the equivalent bending stiffness can be transferred into a translational spring stiffness with simple equations for the deflection w of the beam (with total length l) and spring, where the applied force F corresponds to the rotor thrust force F_T:

$$w = \frac{F\,l^3}{3B_{total}} \quad (beam), \quad F = k\,w \quad (spring) \qquad \Rightarrow \quad k = \frac{3B_{total}}{l^3} \approx 1.98 \cdot 10^6\,\frac{\mathrm{N}}{\mathrm{m}} \tag{A.2}$$

Appendix B. Model Parameters

$N = 3$, $R = 63$ m, $\rho = 1.225\,\mathrm{kg/m^3}$, $J_r = 38759227\,\mathrm{kg\,m^2}$, $J_g = 5025347\,\mathrm{kg\,m^2}$, $k_s = 867637000\,\mathrm{Nm}$, $d_s = 6215000\,\mathrm{Nm\,s}$, $k_B = 40000\,\mathrm{N/m}$, $\alpha = 0.02\,\mathrm{m^{-1}}$, $k_T = 1.98 \cdot 10^6\,\mathrm{N/m}$, $m_{\mathrm{Blade}} = 17740\,\mathrm{kg}$, $m_{\mathrm{Tower}} = 347640\,\mathrm{kg}$, $m_{\mathrm{Rotor}} = 110000\,\mathrm{kg}$, $m_{\mathrm{Nacelle}} = 240000\,\mathrm{kg}$, $\tau_v = 4\,\mathrm{s}$, $m_T = 436865\,\mathrm{kg}$, $m_B = 4435\,\mathrm{kg}$, $d_T = 7 \cdot 10^4 \frac{\mathrm{Ns}}{\mathrm{m}}$, $d_B = 2 \cdot 10^4 \mathrm{Ns/m}$, $r_B = 21.975\,\mathrm{m}$, $\tau = 0.1\,\mathrm{s}$

Appendix C. Observer Gain Matrices

The following weighting matrices ($\mathbf{W}$ for the system states and $\mathbf{R}$ for the system outputs) were used for the optimal LMI observer design: $\mathbf{W} = \mathrm{diag}\left(W_1/\omega_{r,\max}^2 \quad W_2/v_{\max}^2\right)$, $\mathbf{R} = R_1/\omega_{r,\max}^2$, with $W_1 = 15.708$, $W_2 = 60 \cdot 10^7$, $R_1 = 0.157$ and the estimated maximum values $v_{\max} = 60\,\mathrm{m/s}$, $\omega_{r,\max} = 1.5708\,\mathrm{rad/s}$ to normalise the chosen weights.

For the optimal LMI design procedure, the initial observer error is needed, which was set to $\mathbf{e}_0 = (0\,0)^T$. This is of course an idealisation. However, as can be seen from the simulation results, the observer is stable also for $\|\mathbf{e}_0\| > 0$. The following observer gain matrices were obtained: $\mathbf{L}_1 = (93.1 \quad 6731.7)^T$, $\mathbf{L}_2 = (93.1 \quad 6731.7)^T$. $\mathbf{L}_1$ and $\mathbf{L}_2$, displayed here with rounded values, are not equal but differ by less than 0.001 %.

References

[1] Takagi T and Sugeno M 1985 *IEEE Transactions on Systems, Man, and Cybernetics* **15** 116–132
[2] Sugeno M and Kang G T 1988 *Fuzzy Sets and Systems* **28** 15–33
[3] Wang H O, Tanaka K and Griffin M F 1996 *IEEE Transactions on Fuzzy Systems* **4** 14–23
[4] Tanaka K and Wang H O 2001 *Fuzzy Control Systems Design and Analysis: A Linear Matrix Inequality Approach* (John Wiley & Sons, Inc.)
[5] Lendek Z, Guerra T M, Babuška R and De Schutter B 2010 *Stability Analysis and Nonlinear Observer Design Using Takagi-Sugeno Fuzzy Models* (Springer-Verlag Berlin Heidelberg)
[6] Georg S and Schulte H 2014 *Intelligent Systems in Technical and Medical Diagnostics* (*Advances in Intelligent Systems and Computing* vol 230) ed Korbicz J and Kowal M (Springer-Verlag Berlin Heidelberg) pp 41–52
[7] Georg S and Schulte H 2013 *International Conference on Control and Fault-Tolerant Systems* (Nice, France) pp 516–522
[8] Ma X, Poulsen N K and Bindner H 1995 Estimation of Wind Speed in Connection to a Wind Turbine Tech. rep. The Technical University of Denmark
[9] Østergaard K Z, Brath P and Stoustrup J 2007 *Journal of Physics: Conference Series* **75**
[10] Gerland P, Groß D, Schulte H and Kroll A 2010 *IEEE Conference on Decision and Control* (Atlanta, USA) pp 4373–4378
[11] Bindner H 1999 Active Control: Wind Turbine Model Tech. rep. Risø-R-920(EN), Roskilde, Denmark
[12] Bianchi F D, De Battista H and Mantz R J 2007 *Wind Turbine Control Systems - Principles, Modelling and Gain Scheduling Design* (Springer-Verlag, London Limited)
[13] Georg S, Schulte H and Aschemann H 2012 *IEEE International Conference on Fuzzy Systems* (Brisbane, Australia) pp 1737–1744
[14] Jonkman J M and Buhl Jr M L 2005 FAST User's Guide Tech. rep. NREL/EL-500-38230, Golden, Colorado
[15] Jonkman J, Butterfield S, Musial W and Scott G 2009 Definition of a 5-MW Reference Wind Turbine for Offshore System Development Tech. rep. NREL/TP-500-38060, Golden, Colorado
[16] Gasch R and Twele J (eds) 2012 *Wind Power Plants* 2nd ed (Springer-Verlag, Berlin, Heidelberg)
[17] Kaiser K 2000 *Luftkraftverursachte Steifigkeits- und Dämpfungsmatrizen von Windturbinen und ihr Einfluß auf das Stabilitätsverhalten* (VDI-Fortschritt-Berichte, Nr. 294, VDI-Verlag Düsseldorf)
[18] Tanaka K and Sano M 1994 *IEEE Transactions on Fuzzy Systems* **2** 119–134
[19] Ekelund T 1994 *IEEE Conference on Control Applications* (Glasgow, UK) pp 227 – 232
[20] Tanaka K and Sugeno M 1992 *Fuzzy Sets and Systems* **45** 135–156
[21] Bergsten P, Palm R and Driankov D 2001 *IEEE International Conference on Fuzzy Systems* (Melbourne, Australia) pp 700–703
[22] Tanaka K, Taniguchi T and Wang H O 1998 *IEEE Conference on Decision and Control* pp 2914–2919
[23] Van der Hooft E L, Schaak P and van Engelen T G 2003 Wind Turbine Control Algorithms Tech. rep. DOWEC-F1W1-EH-03-094/0, ECN-C–03-111
[24] Gasch R, Knothe K and Liebig R 2012 *Strukturdynamik* (Springer-Verlag Berlin Heidelberg)
[25] Bir G 2012 *NWTC Design Codes (BModes by Gunjit Bir). http://wind.nrel.gov/designcodes/preprocessors/bmodes/*